Multipole moments of ^{154}Sm and ^{166}Er by inelastic scattering of 134 MeV protons

R. M. Ronningen, G. M. Crawley, and N. Anantaraman
National Superconducting Cyclotron Laboratory and Physics Department, Michigan State University, East Lansing, Michigan 48824

S. M. Banks, B. M. Spicer, G. G. Shute, V. C. Officer, and J. M. R. Wastell
School of Physics, University of Melbourne, Parkville, Victoria 3052, Australia

D. W. Devins* and D. L. Friesel
Indiana University Cyclotron Facility, Bloomington, Indiana 47405
(Received 16 March 1983)

Inelastic scattering of 134 MeV polarized protons from ^{154}Sm and ^{166}Er has yielded angular distributions of both cross sections and asymmetries for $J^\pi=0^+$ to 6^+ members of the ground state rotational bands. Deformation parameters β_2, β_4, and β_6 have been extracted from an analysis using coupled channels calculations for scattering from a deformed optical potential. The angular distributions of the cross sections have also been compared with an analytic eikonal model of the reaction. Multipole moments of the potential are determined and are compared with similar moments obtained from electromagnetic measurements and other hadron scattering experiments at different energies. A small energy dependence of the moments for ^{154}Sm is observed. Comparisons are also made to moments obtained from Hartree-Fock calculations and from a liquid drop model. The observed hexadecapole moment of ^{154}Sm is consistently higher than the theoretical predictions.

[NUCLEAR REACTIONS ^{154}Sm(p,p'), ^{166}Er(p,p'), $E_p=134$ MeV, polarized beam; enriched targets, magnetic spectrograph (45 keV FWHM): measured $\sigma(E_{p'},\theta)$, $A_y(E_{p'},\theta)$; coupled channels calculations, deduced optical model parameters; comparisons with electromagnetic measurements, (p,p') and (α,α'), Hartree-Fock and liquid drop calculations.]

I. INTRODUCTION

The main interest in studying inelastic hadron scattering on deformed nuclei has been the hope of extracting the shapes of nuclear matter distributions and comparing these with the accurate charge distributions and transition densities obtained from elastic and inelastic electron scattering. Improvements both in the accuracy of the data available and in the reaction codes have led to substantial improvements in the accuracy of the extracted deformation parameters. In addition, the observation by Mackintosh,[1] that the multipole moments of the reaction potential are related by Satchler's theorem[2] to the moments of the underlying matter distribution if the nucleon-nucleon interaction is density independent, has encouraged comparisons of moments over a wide range of energies and particle types. For example, for ^{154}Sm multipole moments have been extracted from proton inelastic scattering[3,4] at 35 and 800 MeV and compared with moments from electron scattering, Coulomb excitation, and inelastic scattering of other hadronic probes. The moments extracted from the recent accurate hadronic data, analyzed in a similar fashion, seem to be quite consistent among themselves and with the values from electromagnetic measurements.

However, Brieva and Georgiev[5] recently pointed out that because of the energy dependence of a potential derived from a realistic nucleon-nucleon interaction, the moments of a potential derived from a standard phenomenological optical model analysis should show an energy dependence. The energy dependence is expected to be greater for the higher order multipole moments and also greater for the moments extracted from the imaginary part of the potential. Since no data were available on deformed nuclei in the region between 50 MeV and about 150 MeV discussed by Brieva and Georgiev, measurements were made on ^{154}Sm and ^{166}Er with 134 MeV protons to explore the moments in this region.

This region of bombarding energy is also interesting because of the expected strong effects of the spin-orbit force on the shape of angular distributions. Such effects are known in the extensive measurements on a range of spherical nuclei showing high spin stretched states.[6] At 35 MeV, spin-orbit forces have been shown[3] to have a noticeable effect on the quality of the fits to the inelastic cross sections, although the spin-orbit interaction did not need to be deformed to give good fits.[7] However, at 800 MeV, the effect of spin orbit forces on the cross sections and extracted moments is rather small.[8] Up to the present, very few asymmetry measurements have been made on deformed nuclei in the rare earth region, and since such measurements would be expected to be particularly sensitive to spin-orbit forces, the present measurements were carried out with a polarized beam to allow asymmetries to be extracted.

Another advantage of the higher bombarding energies is the ability to extract higher order moments of the potential distribution. Up until now most of the measurements

have obtained only quadrupole ("2 λ pole," where $\lambda=2$) and hexadecapole ($\lambda=4$) moments of the distributions. At 134 MeV, the higher angular momentum states are expected to be excited more strongly relative to the lower angular momentum states than at lower bombarding energies. In addition, at higher energies the angular distributions for the higher J states have more structure than at lower energies, which should allow more detailed comparison with the predictions. This is certainly true at 800 MeV bombarding energy, but this is one of the few cases where a hexacontatetrapole ($\lambda=6$) moment has been obtained. Values of β_6 have been extracted in the rare earth region using inelastic alpha-particle scattering.[9] Since all reported values were either zero or negative, the trend of β_6 values predicted by Nilsson *et al.*[10] does not seem to be followed in this region. It would certainly be of interest to extend measurements of such higher order deformations, to check the values so as to provide accurate data for theoretical predictions of such deformations. In the present experiment, therefore, we chose two targets, ^{154}Sm and ^{166}Er. The former has been extensively studied and is known to have a reasonably large hexadecapole moment. On the other hand, ^{166}Er has a smaller hexadecapole moment and therefore the inelastic scattering might be more sensitive to the higher ($\lambda \geq 6$) moments. Calculations by Nilsson *et al.*,[10] for example, predict opposite signs of β_6 values for ^{154}Sm and ^{166}Er.

Another interesting theoretical development which recently appeared is an analytic approach to inelastic scattering calculations described in a series of papers by Amado and his collaborators.[11–15] These calculations use an eikonal approximation and present simple analytic forms for cross sections both for one- and two-step processes in terms of the elastic scattering cross section. This method is particularly interesting since in principle it should allow one to estimate transition strengths for higher spin states in heavy nuclei without the very large amounts of computing time required by the usual distorted wave coupled channels codes. We will therefore also compare our measurements with some predictions from this analytic theory.

II. EXPERIMENTAL PROCEDURE

The experiment was carried out using a polarized proton beam of energy 133.9±0.1 MeV from the Indiana University Cyclotron Facility. The proton polarizations were between 68% and 73% for spin up, and between 81% and 86% for spin down. The polarization was reversed every 30 sec during a run to help minimize systematic errors. The polarization was measured periodically every three or four hours by scattering from a helium target and was found to be quite stable with time. The actual time dependence of the polarization was determined, and interpolated values were used in analyzing the data obtained in each run.

Outgoing protons were momentum analyzed by the QDDM magnetic spectrometer and were detected in a helical wire counter[16] backed by two plastic scintillators. After careful adjustment of the beam, the overall energy resolution obtained was about 45 keV full width at half maximum (FWHM). The targets consisted of self-supporting foils of enriched isotopes (^{154}Sm99%; $\rho\Delta x = 10.5\pm0.9$mg/cm^2 and ^{166}Er96%; $\rho\Delta x = 3.31\pm0.16$ mg/cm^2). The absolute cross sections were determined by normalizing to the calculated elastic scattering cross section between laboratory angles of 20° and 36°. In this region the calculated cross section is fairly insensitive to the values of the parameters of the optical potential and the value of β_2. For example, a 20% change in β_2 gives only a 3% change in the value of the elastic scattering cross section. The optical potential used was the global, spherical potential determined for energies similar to ours[17] but with deformation parameters "βR" scaled from either a previous study[3] of ^{154}Sm, or from Coulomb excitation studies[18] for ^{166}Er. The uncertainty in this determination was estimated to be about ±8%.

Spectra of protons scattered from ^{154}Sm and ^{166}Er with spin up and spin down at an angle of 47.5° are shown in Fig. 1. Note that the ground state and first excited 2^+ state are quite well resolved even though the separation is only 82 and 81 keV, respectively. The 0^+, 2^+, 4^+, and 6^+ members of the ground state band are cleanly separated from other states. However, the 8^+ states of the ground band in both nuclei are not resolved from neighboring states. In ^{154}Sm, a 1^- state occurs within 18 keV of the 8^+ state; in ^{166}Er the 4_2^+ state is 45 keV from the 8_1^+ state. These states are not readily resolvable and are therefore not included in the coupled channels analysis.

Cross sections and asymmetries were measured for ^{154}Sm from 22.5° to 77.5° and for ^{166}Er from 22.5° to 70° in the laboratory in 2.5° steps. Since the greatest uncertainties in the cross sections extracted from these spectra with many close lying states arise because of the necessity to peak strip and not from the statistics, two completely independent analyses of all the spectra were made, one at Michigan State University (MSU) using the code SCOPEFIT and one at the University of Melbourne using the code MATILDA. The results of these two programs were generally in good agreement, although occasionally discrepancies did arise. After these were resolved, the final data were obtained by averaging the two analyses with the errors reflecting the agreement between the two analyses and the ease of peak stripping as well as the statistics. For the 0^+ and 2^+ cross sections, a 5% stripping uncertainty was added in quadrature with the average error obtained from the two independent analyses. For the 4^+ and 6^+ cross sections, a 5% stripping uncertainty was also added for angles above 40°. However, for smaller angles, a 10% uncertainty was added in quadrature.

The angular distributions of the cross sections and asymmetries for the 0^+, 2^+, 4^+, and 6^+ states are shown in Figs. 2–4. One striking feature of the data is the strong oscillation observed in both differential cross sections and asymmetries, even for the 6^+ states. The cross sections all decrease rapidly with angle. For example, the 2^+ cross section changes by almost four orders of magnitude between 22.5° and 77.5°. Another notable feature of the data is that while the angular distributions for the 2^+ states for these two nuclei are very similar, and the 4^+ angular distributions are fairly similar (especially beyond 30°), the 6^+ angular distributions are quite dissimilar. Not only are the two 6^+ angular distributions not in phase, but the magnitude of the cross section for ^{154}Sm is twice the magnitude of the cross section for scattering to the 6^+ state for ^{166}Er. The asymmetries are quite struc-

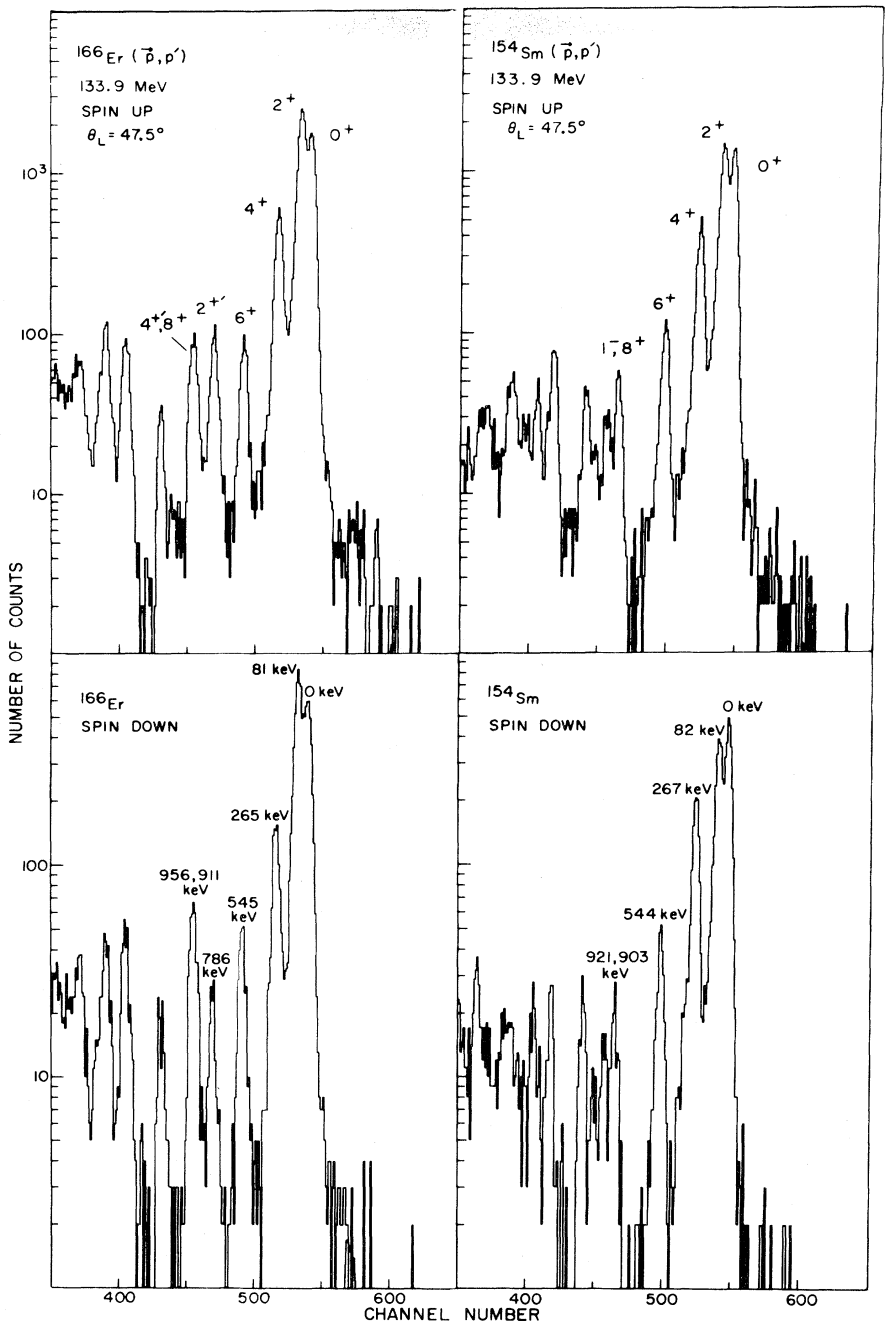

FIG. 1. Spectra of polarized protons at 133.9 MeV elastically and inelastically scattered from ^{154}Sm and ^{166}Er into the laboratory angle of 47.5°. The upper panels are for one polarization direction, protons with "spin up," and the lower panels are for protons polarized to have "spin down." The states of interest to this study are labeled by their spins and parities, J^{π}, in the upper panels, and by their energies in the lower panels.

tured and are positive and large, especially when compared to those for proton scattering on ^{208}Pb at a similar bombarding energy.[17] There are also some phase differences between the analyzing powers for states with the same J^{π} in the two nuclei.

III. ANALYSIS

The data were analyzed using a deformed optical model (DOM) with the coupled channel code ECIS (Ref. 19), which included a deformed full-Thomas spin-orbit term,[20] and employed relativistic kinematics. As is common with such analysis, we assumed that the nuclear states are members of a $K=0$ rotational band. All nonzero couplings between the 0^+ through 8^+ states involving β_2, β_4, and β_6 deformations were included in the coupled channels space, except as specified below. The nuclear potential was assumed to have the standard Woods-Saxon shape with the deformation parameters β_λ introduced in the usu-

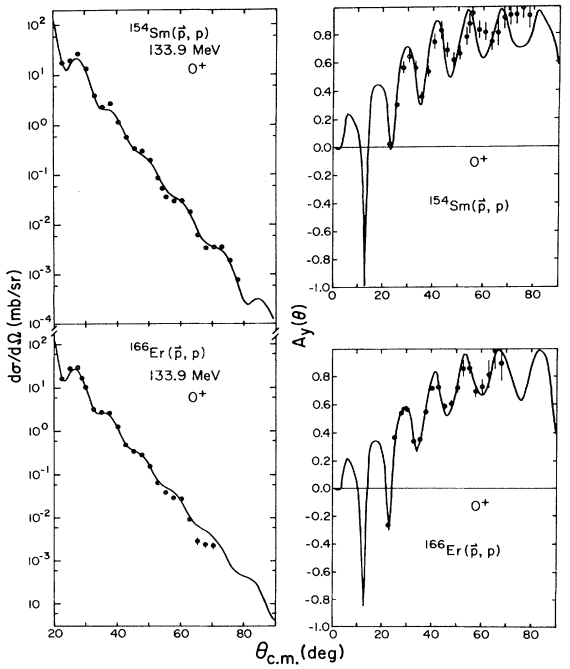

FIG. 2. Comparison of measured (solid symbols) and calculated (solid lines) differential cross section and asymmetry angular distributions for elastic scattering of polarized protons at 133.9 MeV from ^{154}Sm and ^{166}Er. The calculations are described in the text (Sec. III) and are "best fits" when the $\beta_\lambda^{R,I}$ values are allowed to differ from the β_λ^{SO} values. The parameters are given in Table I as case A. Relative errors on the data points are shown by vertical bars where they exceed the size of the symbols.

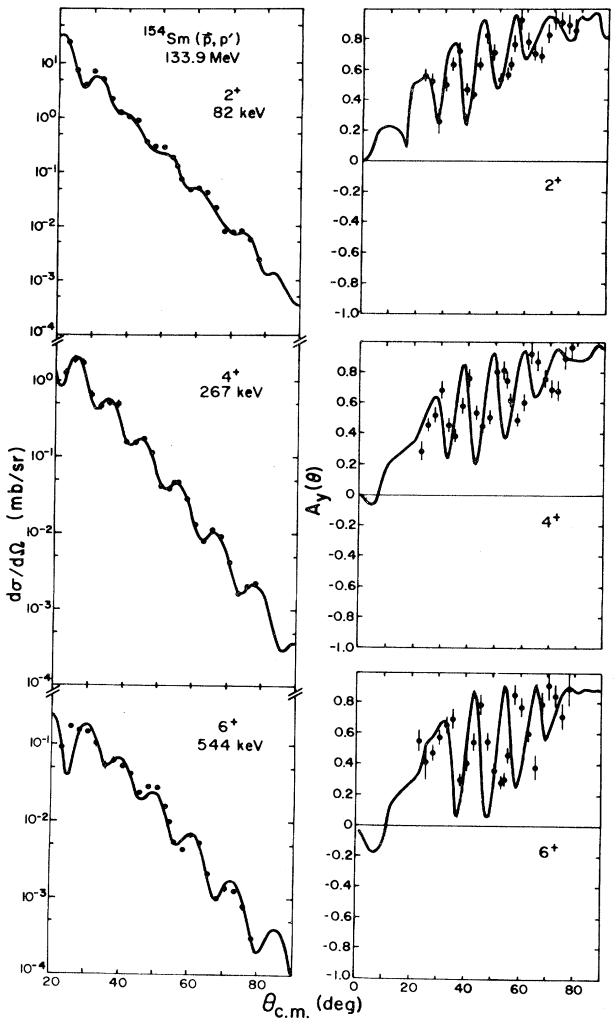

FIG. 3. As for Fig. 2 except the data and calculations are shown for the excited states in the ground band of ^{154}Sm with $J^\pi=2^+$, 4^+, and 6^+.

al way by replacing real, imaginary, and spin-orbit radii by

$$R(\theta)=r_0A^{1/3}\left[1+\sum_\lambda \beta_\lambda Y_{\lambda 0}(\theta)\right].$$

Because of the complicated nature of the χ^2 surface and the interdependence of parameters, the search procedure was carried out as follows. The 0^+, 2^+, and 4^+ angular distributions and asymmetries were used to carry out searches on the optical parameters and β_2 values, leaving the value of β_4 set at some reasonable, previously determined value. The initial values of the optical potential parameters were taken from the systematic studies of Nadasen *et al.*[17] During these searches, the potential depths were varied independently of the corresponding radii to avoid the well-known V-r ambiguity. In the case of ^{154}Sm, the radii were left fixed. When the optical potentials and β_2 value were reasonably well established, then the coupled channels space was extended to include the 6^+ state, and the β_4 deformation was searched on. Couplings to the 8^+ state were included when searches on β_6 deformations were made. Finally, when the parameters appeared to be reasonably stable, a complete search including all deformations and the optical potentials was carried out to obtain the final parameters including uncertainties. The code ECIS gives an uncertainty for each varied parameter which is related to the variation of χ^2. The uncertainties are derived from the inverse of the matrix of second derivatives of χ^2 with respect to the varied parameters, and account for correlations between these parameters. The final values of both the optical parameters and the β_λ's are given in Table I. Note that for both nuclei the β_λ for the real potential, β_λ^R, were always smaller than the β_λ^{SO} for the spin-orbit potential. However, the deformation lengths (βR) of the spin-orbit term agree with those of the real term, except for the $\lambda=4$ case in ^{166}Er.

In order to test the effect of spin-orbit terms, two other calculations were done. In the first, a similar search for the one described above was carried out, but in this case forcing $\beta_\lambda^R=\beta_\lambda^{SO}$ for all λ's (β_λ^I was always kept equal to β_λ^R). The final results of this search are also given in Table I. With this constraint it was not possible to obtain such good fits to the cross sections or analyzing powers. For both nuclei the values of the β_λ's obtained in this search were intermediate between the values obtained with $\beta_\lambda^R\neq\beta_\lambda^{SO}$.

Finally, a search was made without including the spin-orbit potential. In contrast to the case[8] at 800 MeV, the

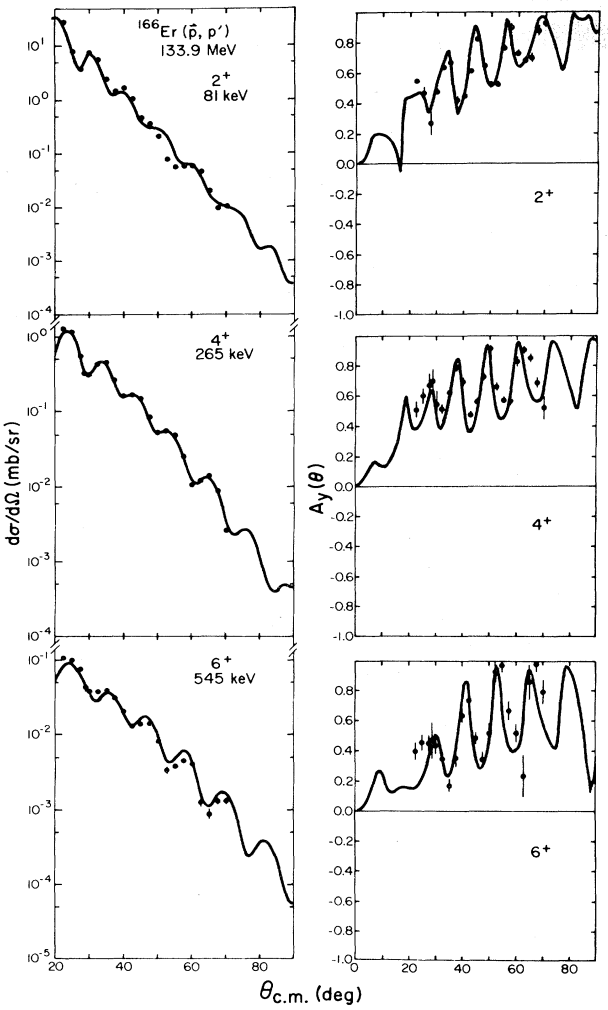

FIG. 4. As for Fig. 3 except for ^{166}Er.

fits to the cross sections were noticeably worsened (see Fig. 5) and the values of the β_λ's were changed significantly, illustrating that at 134 MeV the inclusion of the spin-orbit term is extremely important.

One other feature of the fitting procedure deserves comment. We had hoped that the asymmetries would give better constraint on the values of the spin-orbit potential and deformations. While the fits to the asymmetries were improved slightly by allowing the spin-orbit parameters to vary independently, they did not appear to be significantly more sensitive than the cross sections themselves. In all cases the fits to the asymmetries were somewhat out of phase, with the effect increasing for the higher J states and at larger angles for all J values. Because of this phase slip, a search was also made on the ^{154}Sm data which weighted the cross sections much more strongly than the asymmetries, to be sure that there was no biasing of the results due to the phase shift in the asymmetry data. This search gave very similar results to the earlier search. We therefore conclude that, possibly because we are unable to get a very good fit to the asymmetries, they do not add

TABLE I. Deformed optical model parameters.

Target		V (MeV)	r_R (fm)	a_R (fm)	W (MeV)	r_I (fm)	a_I (fm)	V_{SO}^R (MeV)	W_{SO}^I (MeV)	r_{SO} [c] (fm)	a_{SO} [c] (fm)	β_2^R	β_4^R	β_6^R	β_2^{SO}	β_4^{SO}	β_6^{SO}
^{154}Sm	Case A [a]	24.15	1.210	0.790	5.95	1.393	0.566	2.82	−1.19	1.092	0.652	0.281	0.062	0.009	0.291	0.071	0.007
												(7)	(5)	(3)	(8)	(7)	(7)
^{154}Sm	Case B [b]	25.42	1.210	0.770	6.68	1.393	0.590	2.37	−1.18	1.092	0.630	0.289	0.068	0.010			
^{166}Er	Case A	23.34	1.226	0.756	6.96	1.357	0.651	2.95	−0.84	1.079	0.640	0.276	0.009	−0.007	0.308	0.030	−0.007
												(6)	(5)	(2)	(9)	(6)	(3)
^{166}Er	Case B	23.57	1.222	0.768	6.57	1.357	0.547	2.63	−0.93	1.079	0.599	0.298	0.010	−0.004			

[a]For case A: $\beta_\lambda^R = \beta_\lambda^I \neq \beta_\lambda^{SO}$. Errors for the β_λ are given in parentheses and represent the uncertainties in the last significant digit. These errors were used for the errors in the moments presented in Table II.

[b]For case B: $\beta_\lambda^R = \beta_\lambda^I = \beta_\lambda^{SO}$.

[c]In the case of ^{166}Er the spin-orbit radius and diffuseness are for the real potential only. The imaginary potential radii are 1.088 fm (cases A and B). The diffuseness values are 0.530 fm (case A) and 0.599 fm (case B).

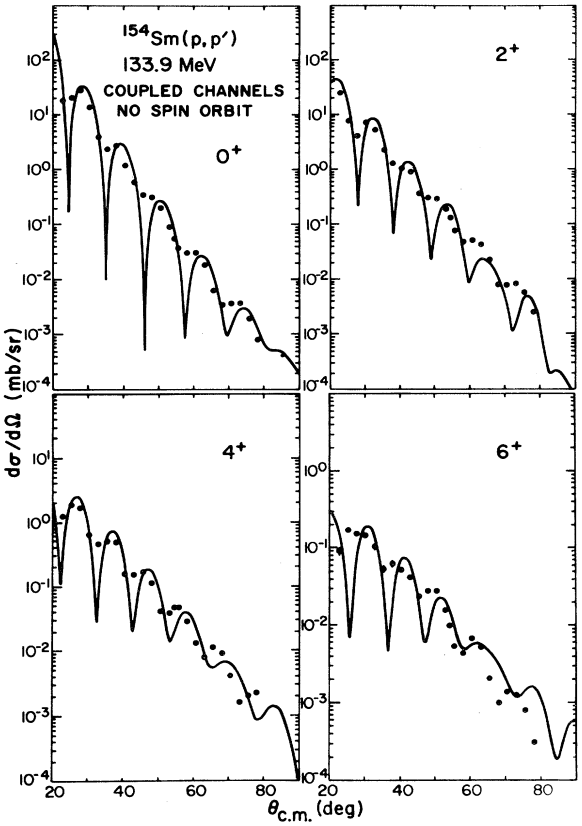

FIG. 5. Comparison of measured (solid symbols) and calculated (solid lines) differential cross sections for elastic and inelastic scattering of polarized protons at 133.9 MeV from ^{154}Sm. The calculations did not include the spin-orbit interaction, and are discussed in Sec. III.

substantially to the information obtained from the cross section measurements.

IV. EIKONAL METHOD

The eikonal approximation is often used to describe high energy hadron-nucleus scattering. Recently, Amado and co-workers[11] obtained analytic expressions for the eikonal integrals using the method of stationary phases. Making the reasonable assumption that the transition density was local and surface peaked, they showed that the scattering was dominated by the geometry of the nucleus. Since both elastic and inelastic scattering were formulated similarly, Amado *et al.*[12] also pointed out that the cross section for inelastic scattering could be formulated directly in terms of the elastic scattering cross section. An advantage of such data to data formulae is that they automatically correct for some effects which are neglected in the derivation.

Amado *et al.*[13] also extended the method to two-step processes in inelastic scattering and derived data to data relations relating two-step cross sections to the elastic scattering cross section in a way similar to the one-step calculation. In the same paper they derived a simple envelope test for the order of the dominant process.

While the method of Amado *et al.* is expected to work best at high bombarding energies and in fact has been applied to some data at 800 MeV, those authors suggest that it may be valid in the region between 100 and 200 MeV. It would be very useful to be able to use the theory in this region because in principle it allows one to extend the calculations to higher spins, which are impossible to treat with a complete coupled channels code because of the very long computing time involved.

As a first step, a qualitative comparison of the variation of the cross sections for the 2^+, 4^+, and 6^+ states was made with one-, two-, and three-step envelope functions as shown in Fig. 6. The functional form is given by

$$E_n = q^{2n} e^{-2\pi\beta q} ,$$

where n is the step order, q is the momentum transfer, and β is the diffuseness parameter in the usual Fermi distribution for the nuclear density. The first order function matches the slope of the 2^+ angular distributions for both ^{154}Sm and ^{166}Er very well, which gives one confidence in the approach. The slope of the 4^+ cross sections, however, matches the two-step function better than the one-step function, suggesting a dominance of a two step excitation of 4^+ states. The slope of the 6^+ angular distributions also matches the two-step function. Again, the implica-

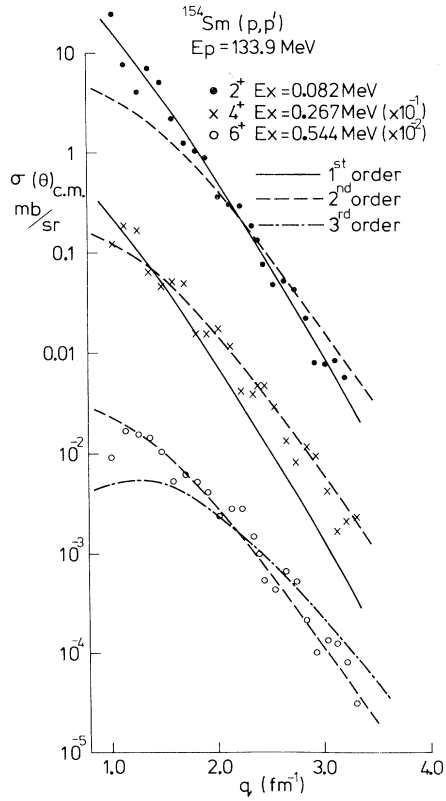

FIG. 6. Comparison of experimental differential cross sections (symbols) as a function of momentum transfer (to $J^\pi = 2^+$, 4^+, and 6^+ states in ^{154}Sm) to one-, two-, and three-step envelope functions as described in Sec. IV. Only the slopes of the calculated curves have significance in comparisons to the data.

tion is that the 6^+ states are excited through either the $0^+ \rightarrow 2^+ \rightarrow 6^+$ or $0^+ \rightarrow 4^+ \rightarrow 6^+$ paths or possibly through both paths but with little strength either in the direct $0^+ \rightarrow 6^+$ or $0^+ \rightarrow 2^+ \rightarrow 4^+ \rightarrow 6^+$ paths.

In more detail, the cross sections for the 4^+ states in both ^{154}Sm and ^{166}Er are compared with both one- and two-step calculations [Eq. (2.22) of Ref. 13] in Fig. 7. The latter calculation used the experimental elastic scattering differential cross section and the $B(E2)$'s for the $0^+ \rightarrow 2^+$ and $2^+ \rightarrow 4^+$ transitions as input. It should be noted that, as pointed out by Haber and Sparrow,[14] the transition strength measured in intermediate energy hadron scattering (a high momentum transfer measurement) should not be expected to be the same as the transition strength measured by the $B(EL)$ values for electromagnetic transitions, which are measurements at essentially zero momentum transfer. Consequently, these calculations using electromagnetic $B(EL)$ values as input can be regarded only as a semiquantitative guide. With the same restriction in mind, a one-step calculation of the $0^+ \rightarrow 4^+$ transition using Eq. (2.51) of Ref. 12 is also shown in Fig. 7 for completeness.

For ^{154}Sm, the two-step calculation gives reasonable qualitative agreement with the data, although the calculation tends to slip out of phase with the data for $q \gtrsim 2.2$ fm^{-1}. The one step calculation appears to be important only for $q \lesssim 1.5$ fm^{-1}. The incoherent addition of one- and two-step cross sections also matches the data fairly well. For ^{166}Er, where the one-step process is very weak [since $B(E4)$ is very small], the two-step calculation alone gives a fairly reasonable fit to the experimental data, although again there is a slippage in phase beyond a momentum transfer of about 2.2 fm^{-1}. Considering the simplicity of the analytic formulation and the lack of adjustable parameters, the agreement with the data is quite good.

The general slope of the 6^+ angular distributions suggests a dominance of two step processes; therefore such calculations were done for both ^{154}Sm and ^{166}Er and the results are shown in Fig. 8. Here, as before, the $B(E2)\uparrow$ values were taken from γ-ray data, and the $B(E4)\uparrow$ value from inelastic electron scattering.

In the case of ^{166}Er, the comparison of the experimental data with a calculation of the $0^+ \rightarrow 4^+ \rightarrow 6^+$ two-step reaction path indicated that the phases are approximately correct, but, as was the case with the two-step processes to the 4^+ states, there is a tendency for the phase to slip at the higher momentum transfers. More importantly, the absolute magnitude of this calculated cross section is about a factor of 2 less than that of the experimental data, indicating that the $0^+ \rightarrow 2^+ \rightarrow 6^+$ reaction path is about as important as the $0^+ \rightarrow 4^+ \rightarrow 6^+$ path for which the calculation was made. From this semiquantitative result, it is possible to estimate the $B(E4)\uparrow$ value for the $2^+ \rightarrow 6^+$ transition as about 0.05 e^2b^4, which is very near the rotational model value of 0.047 e^2b^4.

The results of the two-step process calculations for population of the 6^+ state of ^{154}Sm differ in two important

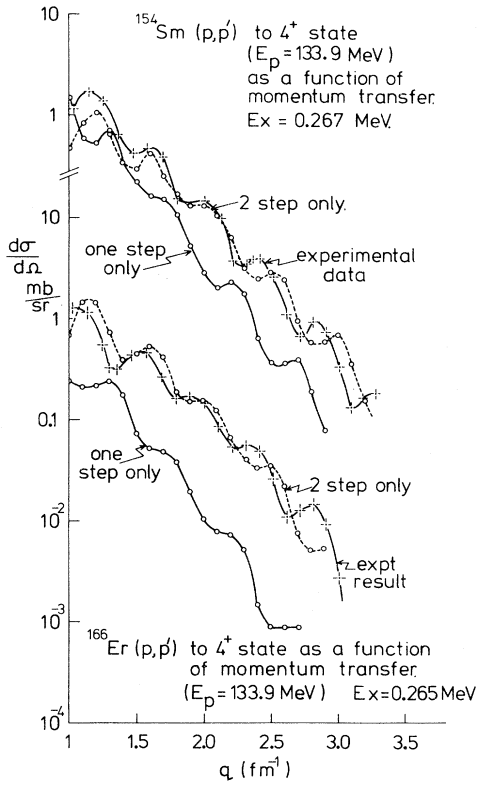

FIG. 7. Comparison of experimental differential cross sections (crosses) for $J^\pi = 4^+$ states in ^{154}Sm (upper curves) and ^{166}Er (lower curves) as a function of momentum transfer to calculations (open symbols) involving one- and two-step processes as described in Sec. IV. The lines through both the data and calculations are to guide the eye.

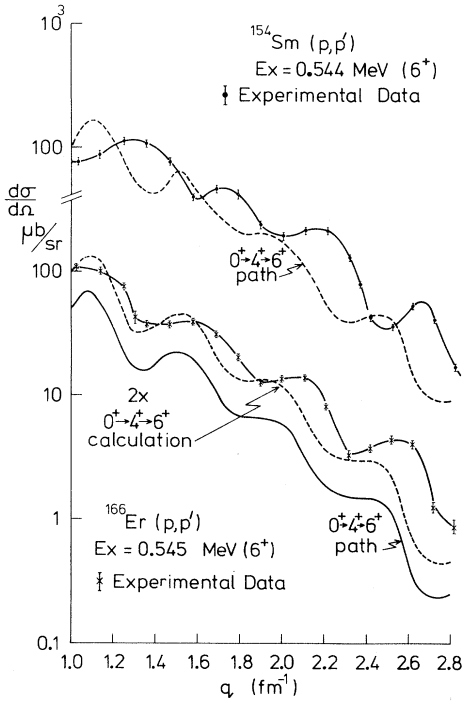

FIG. 8. As for Fig. 7 except for $J^\pi = 6^+$ states. Only symbols for experimental points are shown.

respects from those for ^{166}Er. First, the magnitude of the cross section calculated for the $0^+ \rightarrow 4^+ \rightarrow 6^+$ reaction path is close to that of the experimental data, indicating that, for this nucleus, there is probably little contribution from the $0^+ \rightarrow 2^+ \rightarrow 6^+$ reaction path. Second, the calculated two-step cross section is out of phase with the experimental data for all values of momentum transfer. Indeed, the data are nicely in phase with a one-step calculation for momentum transfer greater than 2 fm^{-1}. Thus we have an experimental differential cross section for ^{154}Sm(p,p')^{154}Sm*(6^+) whose general slope indicates a predominance of two-step processes in the reaction mechanism, yet whose maxima and minima, beyond $q=2$ fm^{-1}, line up with those given in a one-step mechanism calculation. This suggests a significant one-step contribution to this particular reaction channel, and is qualitatively consistent with the relatively large value of q_{60} $(=0.19\pm0.04\ e\text{b}^3)$ given by the coupled channels fitting of the data. However, the expression given by Amado, McNeil, and Sparrow[13] for the relative magnitudes of the one- and two-step contributions indicates that the one-step contribution is less than one-third in amplitude for all values of momentum transfer for which data were obtained. This proportion is not enough to give a calculated result which agrees in phase with the experimental data. The differential cross section for inelastic scattering to the 6^+ state is thus not understood at present.

Even more recently a paper appeared[15] which gives analytic expressions for multistep processes in hadron-nucleus scattering which should, in principle, be even more appropriate for the strongly deformed ^{154}Sm and ^{166}Er cases. However, we have not yet applied these to the present data, since that would require more extensive numerical calculations which were considered to be beyond the scope of the present work.

V. DISCUSSION

The comparison of the results of the DOM analysis with the experimental data allows the extraction of the deformation parameters β_λ defined earlier. The best fit optical parameters and the β_λ's are listed in Table I. However, such β_λ's are not readily comparable between different reactions or even for the same reaction at different energies because of the different properties of the probes. Mackintosh has pointed out,[1] using a result first derived by Satchler,[2] that provided the DOM potential can be derived from a "normal" folding model, then the normalized multipole moments of the nuclear matter distribution are equal to the normalized multipole moments of the folded potential, independent of the range of the potential. A normal folded potential is one where the interaction is central, scalar, and independent of the local nuclear density and of the local energy of the scattered particle within the nucleus. Thus the multipole moments of the DOM potential should be comparable for different probes, and even with electromagnetic measurements, provided that the matter and charge distributions of the nucleus are the same. This, of course, is one of the interesting questions which may be answered by such a comparison. Mackintosh concluded that the comparison between moments from (p,p') and electromagnetic measurements worked well for light nuclei with $N=Z$, where proton and neutron distributions are certainly the same. However, the folding model did not appear to work for the (α,α') reaction. In addition, he concluded tentatively on the basis of measurements available at the time that at least the hexadecapole moments of the matter distribution for heavier nuclei seemed to be smaller than those of the charge distribution.

More recently Brieva and Georgiev[5] carried out a folding procedure using the Hamada-Johnston nucleon-nucleon interaction and included exchange effects to derive a "realistic" scattering potential. They concluded that the current data suggested similar neutron and proton moments but that there should be some noticeable energy dependence in the multipole moments of the optical potential, which is greater for the higher multipoles.

In the light of these predictions it is interesting to compare our results with those of the previous (p,p') and (α,α') measurements at different energies and with electromagnetic measurements. Following Mackintosh, we present the moments of the DOM potential obtained from the present data, together with other results, in Table II. We have chosen to present comparisons only with hadron scattering data above 30 MeV, where at least β_4 was determined in the analysis. There are some very nice neutron data[21] excluded by these criteria, but the quadrupole moments from these results were compared with charged particle scattering previously.

In presenting our results, we have used only the real potential for the cases where the real and spin orbit deformations were not constrained to have the same value. This is believed to be the most accurate measure of the real deformation, since the fits to the angular distributions are improved. In addition, there is no obvious *a priori* reason why the SO deformation should necessarily match the real deformation, since the radius parameters are so different.

We have also constrained the β_λ^R to equal the β_λ^I, mainly to reduce the number of variables in the calculation. The radii of the real and imaginary potential forms are different, and, in principle, these deformation parameters may also be different. However, at 134 MeV the angular distributions are better determined by the properties of the real potential than by the imaginary potential, so that it seems reasonable to use the real potential values. This is no longer true at 800 MeV (Ref. 4), where the imaginary potential is much better determined, and, in fact, the moments quoted at 800 MeV are the moments of the imaginary potential.

A. ^{154}Sm

The quadrupole and hexadecapole moments determined by proton scattering at 35, 51, 134, and 800 MeV are reasonably consistent with one another and with the electromagnetic measurements. At 51 and 800 MeV we assume the errors are similar to those for the 35 MeV and the present data at 134 MeV. The present measurement of q_{20} is about 10% higher than all the other measurements, but this is only a difference of about one standard derivation, and so is probably not very significant. The fractional error on the q_{40} is larger than for the q_{20}, but within these uncertainties the values are quite consistent. The calculations of Brieva and Georgiev[5] suggested about a 6% higher q_{20} moment of the potential at 134 MeV than the electromagnetic moments, assuming that the matter

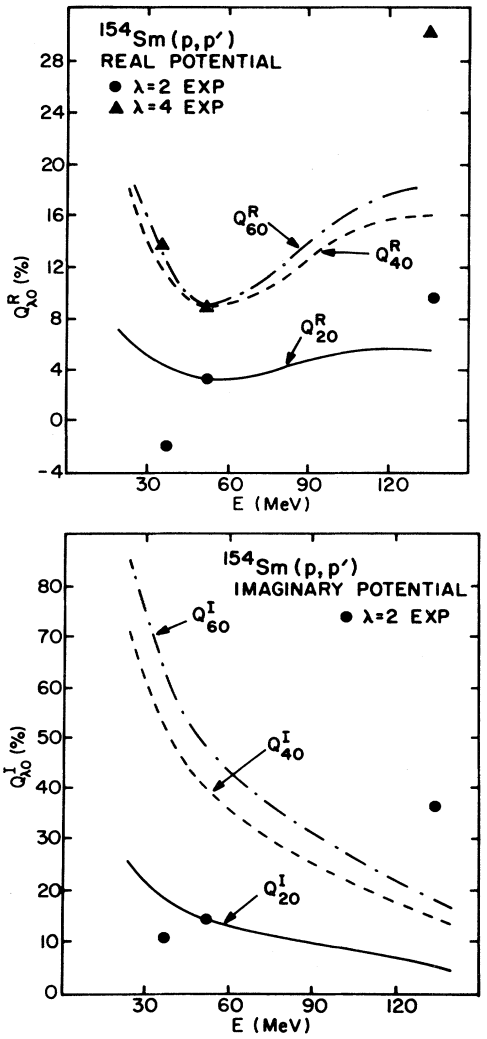

FIG. 9. Comparisons of the percentage differences between experimental multipole moments (closed symbols) from (p,p') reactions and those of a microscopically calculated potential having an underlying density with given multipole moments as a function of incident proton energy. The $Q^{R,I}_{\lambda 0}(E)$ are defined in Sec. V.

and charge distributions are identical and that the electromagnetic measurements give the correct charge distribution. In Fig. 9 we show the percentage variation of the multipole moments of potentials, with respect to those of the underlying nuclear density, for proton scattering at 35, 51, and 134 MeV. The calculations are those of Brieva and Georgiev. The percentage variation is defined as

$$Q^{R,I}_{\lambda 0}(E)=\frac{q^{R,I}_{\lambda 0}(E)-q^{D}_{\lambda 0}}{q^{D}_{\lambda 0}}\times 100\% ,$$

where $q^{R,I}_{\lambda 0}(E)$ are the multipole moments (normalized to mass) of the real and imaginary parts of the phenomenological potential used to fit the scattering data at each energy, and $q^{D}_{\lambda 0}$ are the multipole moments of the matter density used by Brieva and Georgiev ($q^{D}_{20}=5.212$ b, $q^{D}_{40}=1.173$ b^2, $q^{D}_{60}=0.162$ b^3).

Except for Q^R_{20} at 35 MeV the predicted energy dependences for q^R_{20} and q^R_{40} are followed remarkably well, given that the underlying density is correct. Comparisons for Q^R_{60} are not made because the analysis of the 35 MeV data did not include β_6 and because the analysis of the 51 MeV data used negative values of β_6, and our analysis used a positive value of β_6. The omission of a β_6 value of the order we observe will also affect the value of q^R_{40} of the order of 5%. This will cause 20—30% changes in Q^R_{40}. We conclude that the observed energy dependence of the moments may signify that there is not such a simple relation between the moments of the optical potential and the moments of the matter density as we assume, and perhaps density-dependent interaction effects are being observed. However, consistent analyses of existing data, plus data at more points in the energy range considered as well as a greater effort to establish β_6 values, will be necessary to establish quantitatively deviations from the simple assumption above.

For the $Q^I_{\lambda 0}$ the interpretation is even more difficult. The experimental values of Q^I_{20} in Fig. 9 do not follow the predicted trend. Values of Q^I_{40} deviate by factors of up to 2 and thus are not presented. This indicates perhaps that the assumptions about the phenomenological potential, such as equal real and imaginary potential deformations, may be invalid.

No q_{60} moments are given by the electromagnetic measurements, but the various proton measurements seem to be converging on a value around 0.1 e b^3. Again the measurement at 134 MeV is somewhat higher than the measurement at 35 and 800 MeV, and much higher than the (α,α') value. This is because in the analysis of the 35 MeV data no β_6 deformation was used, and negative β_6 values were used in the analysis of the (α,α') (Ref. 9) and 800 MeV proton data.[4] A positive value of β_6 was obtained in the present experiment.

B. ^{166}Er

Comparatively few hadron scattering measurements have been made on ^{166}Er, so that it is only possible to compare our results with the electromagnetic measurements. Both the quadrupole moments and hexadecapole moments measured in the present (p,p') experiment and by inelastic electron scattering or Coulomb excitation measurements agree fairly well. As for ^{154}Sm, the (p,p') experiment gives a q_{20} which is slightly larger than the (e,e') case. However, the q_{40} moment is slightly smaller. No previous measurements of q_{60} have been quoted, although we do extract one from the optical model parameters of Hendrie *et al.*[9] Our value of $+0.01$ eb^3 quoted in Table II is substantially smaller than the value found for ^{154}Sm and is indicative of the nearly zero value of β_4 and the negative value of β_6.

C. Comparison with model calculations

There have been a number of calculations of deformation in the rare earth nuclei using different models. These results are also given in Table II. The most recent is a density dependent Hartree-Fock calculation by Negele and Rinker.[22] Previously, a Hartree-Fock calculation using a

TABLE II. Moments of the DOM potential obtained in this work together with other results.

Target	Reaction	Energy (MeV)	q_{20} (e b)	q_{40} (e b^2)	q_{60} (e b^3)	References
^{154}Sm	(p,p′)	35	2.06 (3)	0.54 (2)		King *et al.* (Ref. 3)
	(p,p′)	51	2.15	0.36	0.07	Wollam *et al.* (Ref. 25)
	(p,p′)	134	2.31 (8)	0.62 (6)	0.19 (4)	This work
	(p,p′)	800	2.12	0.58	0.099	Bartlett *et al.* (Ref. 4)
	(p,p′)	800	2.12	0.54	0.088	Ray (Ref. 8)[a]
	(α,α′)	50	2.38	0.61	0.037	Hendrie *et al.* (Ref. 9)[b]
	(^{3}He,^{3}He′)	41	2.17 (15)	0.47 (6)	0.05 (3)	Palla and Pegel (Ref. 26)[c]
	EM	Av	2.094 (4)	0.588		Ronningen *et al.* (Ref. 18)[d]
	Theory	HF	2.02 p 1.96 n	0.41 p 0.45 n		Negele and Rinker (Ref. 22)
	Theory		2.14 p	0.429 p		Götz *et al.* (Ref. 24)
^{166}Er	(p,p′)	134	2.50 (8)	0.32 (6)	+0.01 (3)	This work
	(α,α′)	50	2.69	0.28	−0.10	Hendrie *et al.* (Ref. 9)[b]
	EM	Av	2.419 (4)	0.24 5 6		Ronningen *et al.* (Ref. 18)[d]
	Theory	HF	2.45 p 2.42 n	0.28 p 0.32 n		Negele and Rinker (Ref. 22)
	Theory	HF	2.46 p	0.326 p		Flocard *et al.* (Ref. 23)
	Theory		2.47 p	0.266 p		Götz *et al.* (Ref. 24)

[a]Same 800 MeV data as Ref. 4 but including spin-orbit potential.
[b]Moments calculated using data of Ref. 9.
[c]Moments calculated using data of Ref. 26.
[d]An average of electromagnetic measurements including measurements added in proof to the compilation in Ref. 18.

Skyrme force was carried out by Flocard *et al.*,[23] but no numbers are given for ^{154}Sm. An alternative approach using a liquid drop model[24] but including shell effects and pairing (Strutinsky method) also gives β_2 and β_4 values for both ^{154}Sm and ^{166}Er. Negele and Rinker give values of the moments of both proton and neutron distributions, and for the hexadecapole moments these differ by 10–20 %.

The measured quadrupole moments agree very well in all cases with the model predictions. However, in ^{154}Sm, the measured hexadecapole moments cluster around 0.60 ± 0.05 e b^2, whereas both theoretical predictions are around 0.4 e b^2. While the measurements are sparse for ^{166}Er, the agreement between theory and measurements is very good, with the value of the hexadecapole moment being about 0.3 e b^2.

There are no predictions for the higher moments in the calculations referred to above. However, an earlier paper by Nilsson *et al.*[10] shows predictions of β_6 across the rare earth nuclei. These have a minimum in β_6 of about -0.025 near $A=170$, with the value changing sign between ^{154}Sm and ^{166}Er (^{154}Sm, $\beta_6\approx+0.005$ and ^{166}Er, $\beta_6\approx-0.012$). The behavior of β_6 and q_{60} across a deformed region can be understood by extending[7] a simple model due to Bertsch.[27] These predictions are consistent with the values of β_6 obtained in the present experiment (Table I). However, further β_6 measurements on more nuclei are needed to confirm the systematic trends predicted.

VI. SUMMARY AND CONCLUSIONS

Measurements of the angular distributions of the cross sections and asymmetries of the inelastic scattering of 134 MeV polarized protons from ^{154}Sm and ^{166}Er show that, indeed, the higher J members of the ground state rotational band are reasonably strongly excited. The angular distributions of the cross sections even for the high J states are quite structured at this energy and can be fitted quite well with coupled channels calculations using the code ECIS. However, the asymmetries are not very well fitted and show a steady slip of phase between data and prediction with increasing scattering angle and increasing J. Spin-orbit effects are very important at these energies and improved fits to the data are obtained when the spin-orbit deformation parameters are allowed to vary independently of the real deformation parameter. In both ^{154}Sm and ^{166}Er, the spin-orbit deformations are larger than the real deformations.

The moments of the deformed optical potential obtained from fitting the data for ^{154}Sm agree quite well with other measurements both for hadronic probes and electromagnetic measurements. A small energy dependence of the moments for ^{154}Sm is observed with the trend between 50 and 134 MeV in the direction predicted by Brieva and Georgiev.[5] No previous proton measurements are available on ^{166}Er, but the values of the quadrupole and hexadecapole moments agree quite well with previous

values from (α,α') (Ref. 9) and Coulomb excitation.[18]

The angular distributions of the cross sections have also been compared with the analytic eikonal model of Amado *et al.*[11] The general slope of the inelastic cross sections for the 4^+ and 6^+ states versus momentum transfer is well represented by $q^4 e^{-2\pi\beta q}$ as suggested by Amado *et al.*[13] for a second order process. Fits to the 4^+ cross sections for both ^{154}Sm and ^{166}Er with a two-step calculation are reasonably good although there is a phase difference at large momentum transfer. Two-step calculations for the 6^+ states suggest that the $0^+\rightarrow 2^+\rightarrow 6^+$ and $0^+\rightarrow 4^+\rightarrow 6^+$ paths are of comparable importance for ^{166}Er, but that the $0^+\rightarrow 4^+\rightarrow 6^+$ path is dominant for ^{154}Sm.

The quadrupole moments for both ^{154}Sm and ^{166}Er agree very well with predictions both of Hartree-Fock[22] and liquid drop Strutinsky calculations,[24] as does the hexadecapole moment for ^{166}Er. However, the experimental hexadecapole moment for ^{154}Sm is about 50% higher than the predictions of either model. Finally, a β_6 deformation parameter was obtained for ^{166}Er. This value together with the ^{154}Sm, β_6 value agrees with the trend suggested by Nilsson *et al.*,[10] but more data are needed to confirm the systematics.

ACKNOWLEDGMENTS

The authors would like to thank Dr. R. Smith for assistance with ECIS calculations and J. J. Stevermer for valuable help in data analysis. This work was partially supported by the U. S. National Science Foundation under Grants PHY80-17605 and INT 82-00250 and the Australian Research Grants Scheme. One of the authors (G.M.C.) also acknowledges financial support from the University of Melbourne and the warm hospitality of the Physics Department during his stay in Melbourne.

---

*Present address: Koppers Process Technology, Norcross, GA 30093.

[1]R. S. Mackintosh, Nucl. Phys. A266, 279 (1976).
[2]G. R. Satchler, J. Math Phys. 13, 1118 (1972).
[3]C. H. King, J. E. Finck, G. M. Crawley, J. A. Nolen, Jr., and R. M. Ronningen, Phys. Rev. C 20, 2084 (1979); C. H. King, G. M. Crawley, J. A. Nolen, Jr., and J. E. Finck, J. Phys. Soc. Jpn. Suppl. 44, 564 (1978).
[4]M. L. Bartlett, G. A. McGill, L. Ray, M. M. Bartlett, G. W. Hoffmann, N. M. Hintz, G. S. Kyle, M. A. Franey, and G. Blanpied, Phys. Rev. C 22, 1168 (1980).
[5]F. A. Brieva and B. Z. Georgiev, Nucl. Phys. A308, 27 (1978).
[6]R. A. Lindgren, W. J. Gerace, A. D. Bacher, W. G. Love, and F. Petrovich, Phys. Rev. Lett. 42, 1524 (1979).
[7]R. M. Ronningen, R. C. Melin, J. A. Nolen, Jr., G. M. Crawley, and C. E. Bemis, Jr., Phys. Rev. Lett. 47, 635 (1981).
[8]L. Ray, Phys. Lett. 102B, 88 (1981).
[9]D. L. Hendrie *et al.*, Phys. Lett. 26B, 127 (1968).
[10]S. G. Nilsson, Chin Fu Tsang, A. Sobiczewski, Z. Szymanski, S. Wychech, C. Gustafson, I.-L. Lamm, P. Möller, and B. Nilsson, Nucl. Phys. A131, 1 (1969).
[11]R. D. Amado, J.-P. Dedonder, and F. Lenz, Phys. Rev. C 21, 647 (1980).
[12]R. D. Amado, F. Levy, J. A. McNeil, and D. A. Sparrow, Phys. Rev. C 22, 2094 (1980).
[13]R. D. Amado, J. A. McNeil, and D. A. Sparrow, Phys. Rev. C 23, 2186 (1981).
[14]H. E. Haber and D. A. Sparrow, Phys. Rev. C 25, 1959 (1982).
[15]R. D. Amado, J. A. McNeil, and D. A. Sparrow, Phys. Rev. C 25, 13 (1982).
[16]V. C. Officer, R. S. Henderson, and I. D. Svalbe, Bull. Am. Phys. Soc. 20, 1169 (1975).
[17]A. Nadasen, P. Schwandt, P. P. Singh, W. W. Jacobs, A. D. Bacher, P. T. Debevec, M. D. Kaitchuck, and J. T. Meek, Phys. Rev. C 23, 1023 (1981); P. Schwandt, H. O. Meyer, W. W. Jacobs, A. D. Bacher, S. E. Vigdor, M. D. Kaitchuck, and T. R. Donoghue, *ibid.* 26, 55 (1982).
[18]R. M. Ronningen, J. H. Hamilton, L. Varnell, J. Lange, A. V. Ramayya, G. Garcia-Bermudez, W. Lourens, L. L. Riedinger, F. K. McGowan, P. H. Stelson, R. L. Robinson, and J. L. C. Ford, Jr., Phys. Rev. C 16, 2208 (1977).
[19]J. Raynal, program ECIS (unpublished).
[20]R. de Swiniarski, Dink-Lien Phaun, and G. Bazieu, Can. J. Phys. 55, 43 (1977).
[21]Ch. Lagrange, J. Lachkar, G. Haouat, R. E. Shamu, and M. T. McEllistrem, Nucl. Phys. A345, 193 (1981); M. T. McEllistrem, R. E. Shamu, J. Lachkar, G. Haouat, Ch. Lagrange, Y. Patin, J. Sigaud, and F. Cocu, Phys. Rev. C 15, 927 (1977).
[22]J. W. Negele and G. Rinker, Phys. Rev. C 15, 1499 (1977).
[23]H. Flocard, P. Quentin, and D. Vautherin, Phys. Lett. 46B, 304 (1973).
[24]U. Götz, H. C. Pauli, K. Alder, and K. Junker, Nucl. Phys. A192, 1 (1972), as given in I. Y. Lee *et al.*, Phys. Rev. C 12, 1483 (1975).
[25]P. B. Wollam, R. J. Griffiths, F. G. Kinston, C. B. Fulmer, J. C. Hafele, and A. Scott, Nucl. Phys. A179, 657 (1972).
[26]G. Palla and C. Pegel, Nucl. Phys. A321, 317 (1979).
[27]G. F. Bertsch, Phys. Lett. 26B, 130 (1968).